

Interfacial synthesis of crystalline two-dimensional cyano-graphdiyne

Zhaohui Zhang,^{a,b} Chenyu Wu,^a Qingyan Pan,^a Feng Shao,^c Qingzhu Sun,^a Siqi Chen,^a Zhibo Li^{a*} and Yingjie Zhao^{a*}

^a College of Polymer Science and Engineering, Qingdao University of Science and Technology, Qingdao 266042, China.

^b College of Materials Science and Engineering, Qingdao University of Science and Technology, Qingdao 266042, China.

^c Department of Chemistry, Faculty of Science, National University of Singapore, 3 Science Drive 3, Singapore 117543.

[*] Corresponding Authors: yz@qust.edu.cn, zbli@qust.edu.cn.

Supporting Information

Table of Contents

1. Supporting Methods

1.1 General materials and methods	S3-S4
1.2 Synthesis	S4-S7
1.3 Electrochemistry	S7
1.4 Stacking mode analysis	S7-S8
1.5 The density functional theory methods	S8
1.6 References	S8-S9

2. Supporting Figures and Legends

Figure S1: Synthetic scheme.	S10
Figure S2: ^1H -NMR of compound A in CDCl_3	S11
Figure S3: ^{13}C -NMR of compound A in CDCl_3	S11
Figure S4: ^1H -NMR of compound B in CDCl_3	S12
Figure S5: ^{13}C -NMR of compound B in CDCl_3	S12
Figure S6: ^1H -NMR of compound C in DMSO	S13
Figure S7: ^{13}C -NMR of compound C in DMSO	S13
Figure S8: ^1H -NMR of compound D in DMSO	S14
Figure S9: ^{13}C -NMR of compound D in DMSO	S14
Figure S10: ^{13}C -NMR of compound F in DMSO	S15
Figure S11: ^1H -NMR of compound G in CDCl_3	S15
Figure S12: ^{13}C -NMR of compound G in CDCl_3	S16
Figure S13: High resolution N 1s XPS spectra of CN-GDY on HMDS modified SiO_2/Si .	S16
Figure S14: a-d SEM images of CN-GDY ; e-h TEM images of CN-GDY	S17
Figure S15: Thickness statistics of different CN-GDY samples.	S17
Figure S16: UV-vis spectrum of the compound G and CN-GDY	S18
Figure S17: Cyclic voltammetry curves(CV) of the compound G and CN-GDY	S18
Figure S18: The mono-layer model obtained by the Forcite module in Materials Studio software packages	S19
Figure S19: Side and top views of CN-GDY	S19
Figure S20: Total charge density distribution with an isovalue of 0.16 electrons/bohr ³ for the isosurfaces	S20
Figure S21: The electron localization function for CN-GDY (001) surface	S20
Figure S22: Side views of the partial density for the top of the valence band with an isovalue of 0.0005 electrons/bohr ³	S21
Figure S23: Side views of the partial density for the bottom of the conduction band with an isovalue of 0.0005 electrons/bohr ³	S21
Figure S24: Raman spectras of the compound G and CN-GDY	S22

1. Supplementary Methods

1.1. Materials and Methods

All reactions were carried out under nitrogen condition unless otherwise noted. ^1H and ^{13}C NMR spectra were performed on 500 MHz spectrometers (Bruker AVANCE-III 500) or 400 MHz spectrometers (Bruker AVANCE NEO 400 Ascend) in the indicated solvents at room temperature. Chemical shifts were reported in δ (ppm) relative to TMS (δ ppm). Unless otherwise indicated, column chromatography was carried out on silica gel (200-300 mesh). Thin-layer chromatography (TLC) analysis was performed on precoated silica gel plates (0.2 mm thick). Scanning electron microscopy (SEM) images were collected using scanning electron microscope (JEOL, JSM-7500F) at an accelerating voltage of 5.0 kV. Transmission electron microscopy (TEM) was performed on a JEM-2100 electron microscope with an accelerating voltage of 200 kV. The UV-vis absorbance was measured by UV spectrometer (HITACHI, 3900). Atomic Force Microscope (AFM) images were recorded on Bruker Multimode 8 AFM with Nanoscope V controller. XPS was performed on a Thermo Scientific ESCALab 250Xi instrument. The parameters were as follows: Al K α (1486.6 eV, 150 W) radiation was used as the X-ray source, the vacuum degree of the chamber was 3.6×10^{-9} mbar and the scan range was -10-1350 eV. The spectra were analyzed using XPSpeak Software. High resolution mass spectra were obtained by ESI mass spectrometer (Bruker Impact II) and the $[\text{M}+\text{H}]^+$ or $[\text{M}+\text{Na}]^+$. Raman spectra was investigated on HORIBA Raman spectrometer (LabRAM HR Evolution), with an excitation wavelength at 532 nm and

spot diameter for 1 μm . Attenuated total reflectance (ATR) FT-IR spectra were recorded on a Bruker Tensor 27 Spectrometer.

Abbreviations. Dichloromethane (DCM), trichloromethane (CHCl_3), Ethanol (EtOH), Potassium Acetate (KOAc), Sodium acetate (NaOAc), Tetrakis(triphenylphosphine)palladium (0) ($\text{Pd}[\text{P}(\text{C}_6\text{H}_5)_3]_4$), Tetrabutylammonium fluoride (TBAF), Cupric Acetate ($\text{Cu}(\text{AcO})_2$), Thin-layer chromatography (TLC), Scanning electron microscopy (SEM), Transmission electron microscopy (TEM), Atomic Force Microscope (AFM).

1.2 Synthesis

Synthesis of 1,3,5-Tribromo-2,4,6-trimethylbenzene (A)

To a 1-L 3-necked flask containing aluminum bromide (0.27 g, 0.001 mol) and bromine (96 g, 0.6 mol) fitted with appropriate vents to accommodate the large quantities of HBr gas produced in this reaction. 1,3,5-trimethylbenzene (12 g, 0.1 mol) was added slowly within 1.5 h at 0 $^\circ\text{C}$. Then the mixture was allowed to warm to room temperature and stirred for 2 days. After the addition of 50 mL water, the crude product was filtered, washed with water and recrystallized from CHCl_3 to give colorless fine needles (23 g, 65%). ^1H NMR (400 MHz, CDCl_3): 2.65(s, CH_3 , 9H). ^{13}C NMR (100 MHz, CDCl_3): 137.0, 125.0, 26.3. MS (ESI): 357.81 $[\text{M}+\text{H}]^+$.

Synthesis of 1,3,5-Tribromo-2,4,6-tris(bromomethyl)benzene (B)

To 1,3,5-tribromo-2,4,6-trimethylbenzene (A) (35.7 g, 0.1 mol) in 150 mL of 1,2-dibromoethane in a 1-L flask equipped with a reflux condenser was added bromine (48 g, 0.3 mol) over a period of 30 min at room temperature. The mixture was heated to

reflux for 20 h. Upon cooling the reaction mixture to r. t. the product precipitates. The crude product was filtered, washed with a small amount of 1,2-dibromoethane and recrystallized from CHCl₃ to give a colorless powder (56 g, 96%). ¹H NMR (400 MHz, CDCl₃): 4.93(s, CH₂, 6H). ¹³C NMR (100 MHz, CDCl₃): 138.0, 128.5, 35.5. MS (ESI): 594.58 [M+H]⁺.

Synthesis of 1,3,5-Tribromo-2,4,6-tris(hydroxymethyl)benzene (C)

To 150 mL of DMF were added 1,3,5-tribromo-2,4,6-tris(bromomethyl)benzene (**B**) (14.9 g, 0.025 mol) and KOAc (14.7 g, 0.150 mol). The mixture was heated to 80 °C for 20 h and then cooled to r. t., treated with 100 mL of water, poured into CH₂Cl₂, and extracted. The organic layer was washed with water, dried with Na₂SO₄. After evaporation of the solvent, the residue was added aq. KOH (14 g, 0.250 mol) and the mixture stirred and heated to 90 °C for 24 h. The reaction mixture was cooled, neutralized, and the colorless solid filtered off and washed with small amounts of MeOH and Et₂O to give the final product (9.2 g, 92%). ¹H NMR (400 MHz, DMSO): 5.26(t, *J* = 5.2 Hz, OH, 3H), 4.90(d, *J* = 5.2 Hz, CH₂, 6H). ¹³C NMR (100 MHz, DMSO): 140.1, 129.0, 65.9. MS (ESI): 405.67 [M+H]⁺.

Synthesis of 2,4,6-Tribromo-1,3,5-benzenetricarbaldehyde (D)

To PCC (56.0 g, 0.60 mol) in CH₂Cl₂ (1.80 L) was added celite (20.0 g) and 4Å molecular sieves (20.0 g), followed by 1,3,5-tribromo-2,4,6-tris(hydroxymethyl)benzene (**C**) (14.0 g, 35.0 mmol). The mixture was stirred vigorously at 25 °C for 2 d, filtered through a pad of silica gel eluting with CH₂Cl₂, and the solvent evaporated to yield pure 1,3,5-tribromo-2,4,6-benzenetricarboxaldehyde as

fluffy white needles (12.0 g, 86%). ¹H NMR (400 MHz, DMSO): 10.11(s, CHO, 3H).
¹³C NMR (100 MHz, DMSO): 192.9, 137.5, 124.1. MS (ESI): 399.53 [M+H]⁺.

Synthesis of 1,3,5-tribromo-2,4,6-tri(hydroxyiminomethyl)benzene (E)

To a solution of 2,4,6-tribromo-1,3,5-benzenetricarbaldehyde (**D**) (4 g, 10 mmol) in 50 mL of EtOH were added NaOAc (4.9 g, 60 mmol) and hydroxylammonium chloride (4.2 g, 60 mmol). The mixture was heated to 60 °C for 2 h, cooled and poured into ice water. The crude product was filtered, washed with EtOH and dried in a vacuum (3.04 g, 69%). Without purification, the obtained solid was directly reacted with the next step.

Synthesis of 1,3,5-Tribromo-2,4,6-tricyanobenzene (F)¹

A solution of 2,4,6-tribromo-1,3,5-tri(hydroxyiminomethyl)benzene (**E**) (4.4 g, 10 mmol) in 50 mL of acetic anhydride was heated to reflux for 6 h. The solvent was removed in vacuo resulting in a brown residue. The crude product was recrystallized from benzene to give a colorless solid (2.4 g, 62%). ¹³C NMR (100 MHz, DMSO): 136.5, 120.8, 115.5. MS (ESI): 390.89 [M+H]⁺.

Synthesis of 1,3,5-tricarbonitrile-2,4,6-tris((trimethylsilyl)ethynyl)benzene (G)²

A mixture of 1,3,5-Tribromo-2,4,6-tricyanobenzene (**F**) (3.8g, 10mmol), tributyl(trimethylsilylethynyl)tin (13.9g, 36mmol), and Tetrakis(triphenylphosphine)palladium (0) (2.3g, 2mmol) in toluene (240mL) was stirred under 95 °C condition for 12 h. After cooling, the solvent was evaporated. Recrystallization of the residue from tetrahydrofuran-methanol gave 1,3,5-tricarbonitrile-2,4,6-tris((trimethylsilyl)ethynyl)benzene (**G**) as a light yellow solid (3.4g, 78.9%). ¹H NMR (400 MHz, CDCl₃): 0.34(s, CH₃, 27H). ¹³C NMR (100 MHz,

CDCl₃): 133.7, 118.7, 117.1, 113.6, 96.3, 0.0. MS (ESI): 442.58 [M+H]⁺.

Preparation of CN-GDYs via liquid/liquid interface³

To a solution of the precursor (Compound **G**) (1.0 μmol) in CH₂Cl₂ (10 ml) was added TBAF (1 M in THF, 10 μL, 10 μmol) into a glass cylinder with a diameter of 40 mm and stirred at room temperature for 3 min in the dark. The solution was then covered with pure water (10 mL) carefully. An aqueous solution (10 mL) of Cu(AcO)₂ (0.05 mg/mL) and pyridine (0.05 M) was added gently to the water phase. The system was kept undisturbed for 5 days in the dark. The upper layer was then replaced with pure water, while the organic phase was replaced with pure CH₂Cl₂. After the removal of both aqueous and organic phases, the resultant **CN-GDY** film was suspended in ethanol. The suspension was cast dropwise on various substrates for measurements.

1.3 Electrochemistry

The reduction potentials of Compound **G** and **CN-GDY** were determined using cyclic voltammetry and differential pulse voltammetry (DPV, scan rate 100 mV/s) vs Fc⁺ / Fc in DCM (supporting electrolyte: 100 mM Bu₄NPF₆, working electrode: Pt, counter electrode: Pt wire, reference electrode: SCE). LUMO energies vs vacuum were calculated from reduction peak in DPV using the equation S1⁴.

$$E_{\text{LUMO}} = -5.1 \text{ eV} - E_{\text{DPV vs (Fc}^+ / \text{Fc)}} \quad (\text{S1})$$

1.4 Stacking mode analysis

Firstly, the single-layer model was obtained from molecular-mechanics-based structure

optimization by the Forcite module in Materials Studio software packages. A space group of P6/mmm was found for this single-layer model (Figure 4). Apparently, the single-layer bears a simulated maximum plane spacing $d_{\max} = d\{100\} = 1.35$ nm. However, d_{\max} determined from the experimental SAED pattern occurred to be $d_{\max} = 0.449$ nm, clearly indicating the presence of a stacking mode generating systematic diffraction distinction. Subsequently, we performed geometrical analysis to uncover this stacking mode. As shown in Figure 4, the 9-fold stacking mode exhibits a $d_{\max} = d_{\{300\}} = 0.476$ nm, in excellent agreement with the experimental $d_{\max} = 0.449$ (relative error $\delta = 5.4\%$), exclusively reflecting a 9-fold stacking mode as presented in Figure 4.

1.5 The density functional theory methods

All the calculations are performed in the framework of the density functional theory with the projector augmented plane-wave method, as implemented in the Vienna ab initio simulation package.⁵ The generalized gradient approximation proposed by Perdew, Burke, and Ernzerhof is selected for the exchange-correlation potential.⁶ The cut-off energy for plane wave is set to 400 eV. The energy criterion is set to 10^{-5} eV in iterative solution of the Kohn-Sham equation. The Brillouin zone integration is performed at the Gamma point. All the structures are relaxed until the residual forces on the atoms have declined to less than 0.03 eV/Å.

1.6 References

1. M. Becker, K. Voss, A. Villinger and A. Schulz, *Zeitschrift für Naturforschung*

- B*, 2012, **67**, 643-649.
2. Y. Ma, X. Zhang, S. Stappert, Z. Yuan, C. Li and K. Mullen, *Chem. Commun.*, 2017, **53**, 5310-5313.
 3. R. Matsuoka, R. Sakamoto, K. Hoshiko, S. Sasaki, H. Masunaga, K. Nagashio and H. Nishihara, *J. Am. Chem. Soc.*, 2017, **139**, 3145-3152.
 4. Y. Zhao, G. Huang, C. Besnard, J. Mareda, N. Sakai and S. Matile, *Chem. Eur. J.*, 2015, **21**, 6202-6207.
 5. G. Kresse and D. Joubert, *Physical Review B*, 1999, **59**, 1758-1775.
 6. K. B. John P. Perdew, Matthias Ernzerhof, *Physical review letters*, 1996, **77**, 18.

2. Supporting Figures and Legends

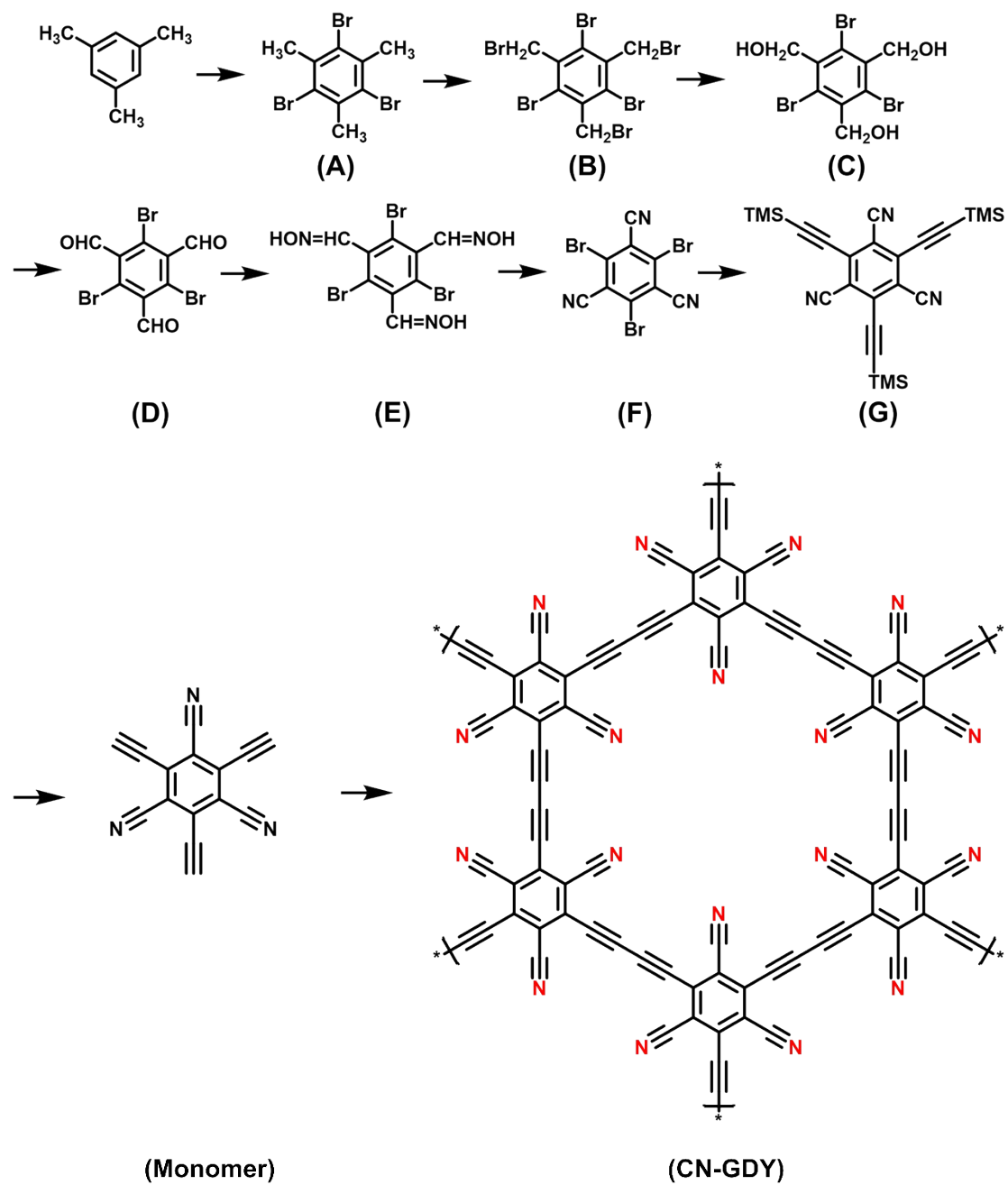


Figure S1. Synthetic scheme for the polymer CN-GDY.

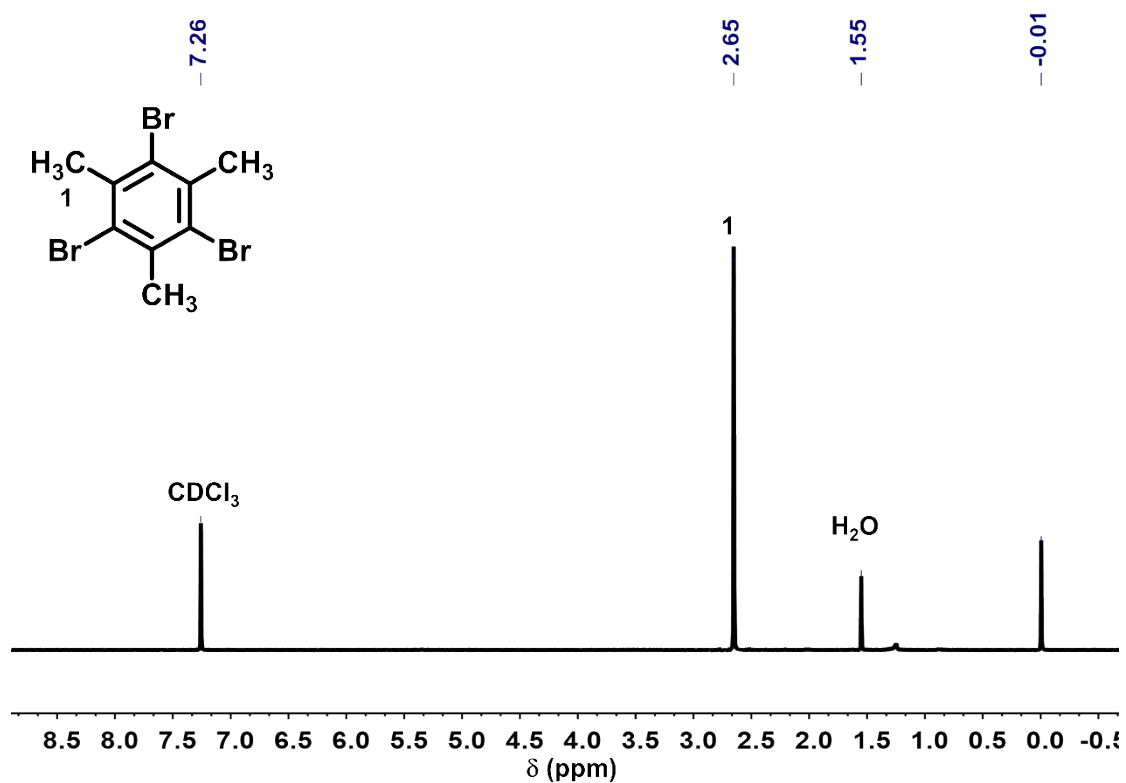


Figure S2. $^1\text{H NMR}$ (400 MHz) spectrum of compound A in CDCl_3 .

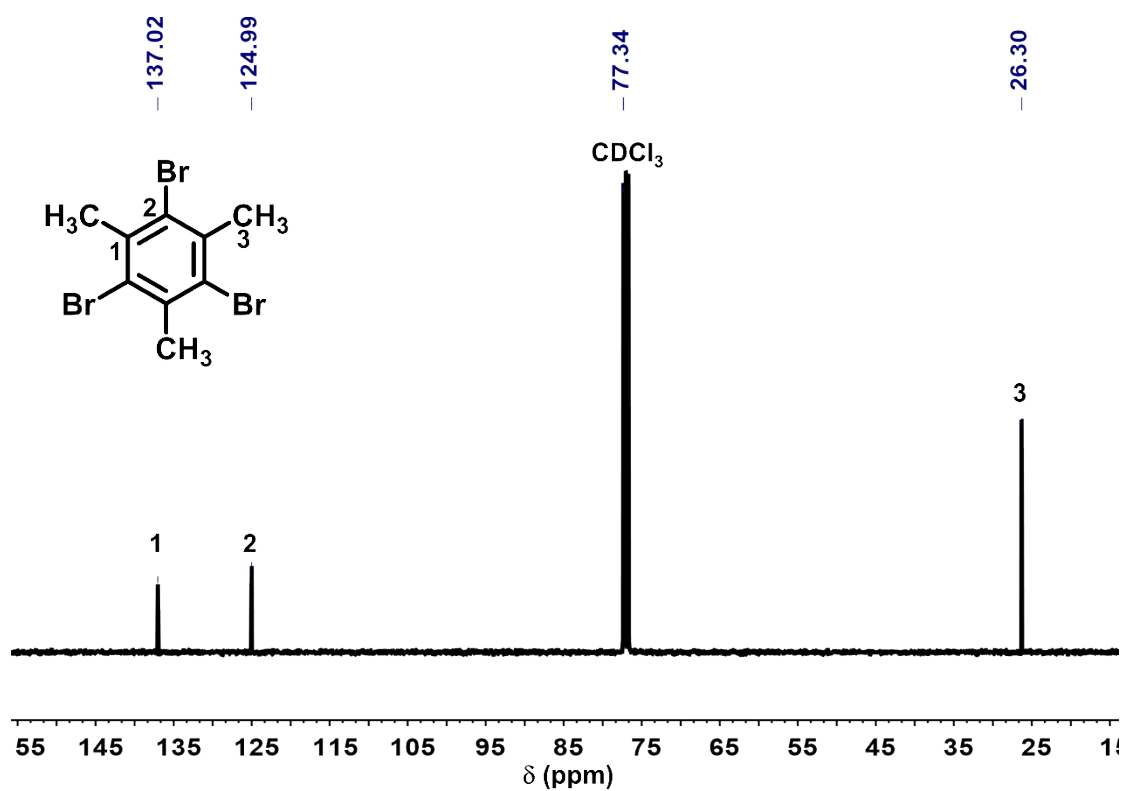


Figure S3. $^{13}\text{C NMR}$ (100 MHz) spectrum of compound A in CDCl_3 .

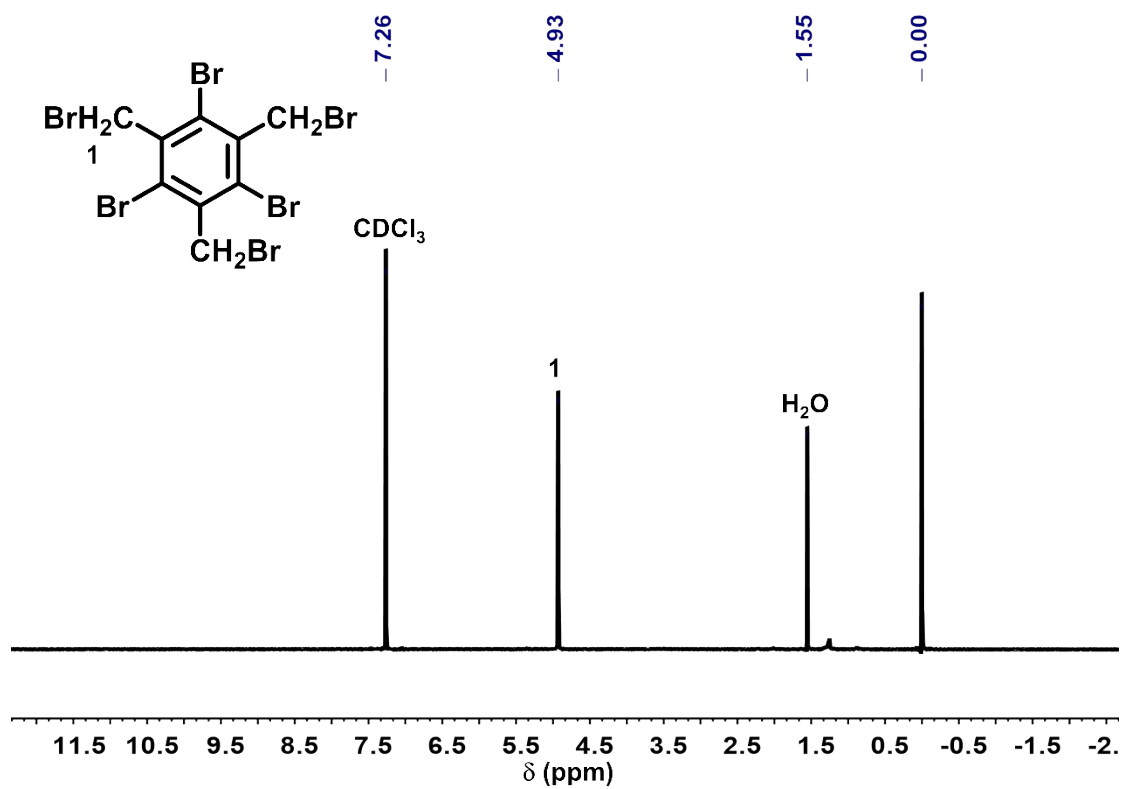


Figure S4. ^1H NMR (400 MHz) spectrum of compound **B** in CDCl_3 .

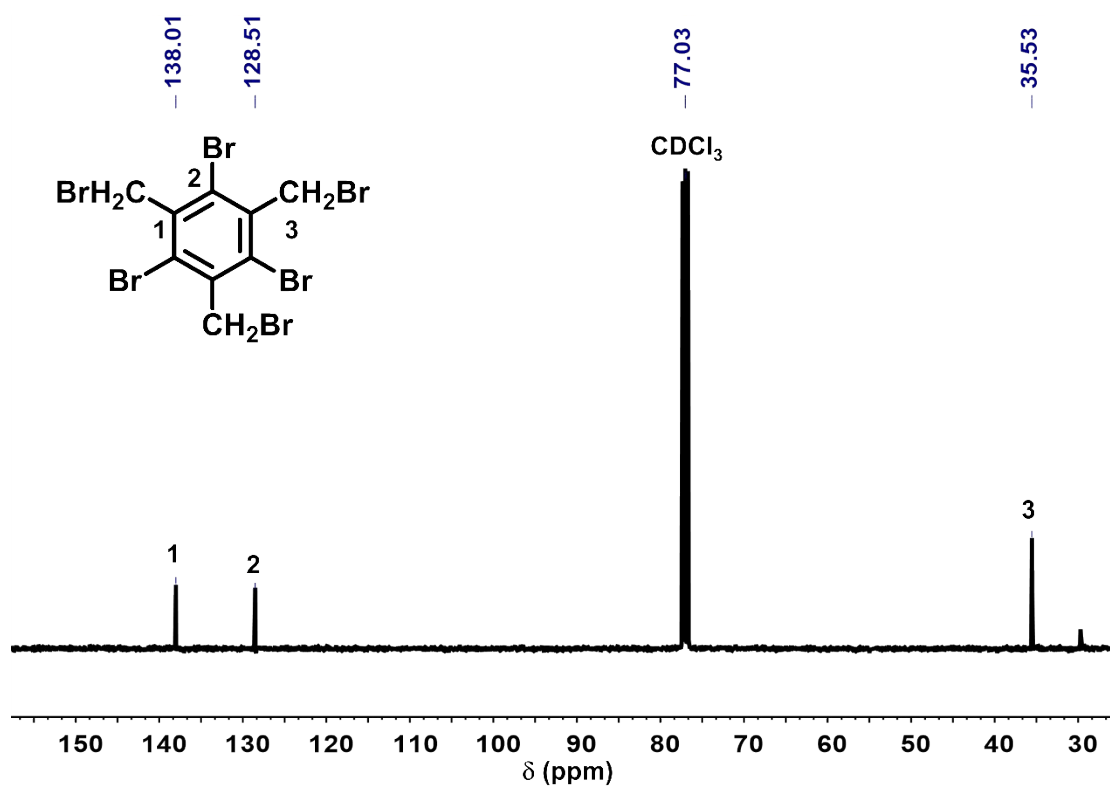


Figure S5. ^{13}C NMR (100 MHz) spectrum of compound **B** in CDCl_3 .

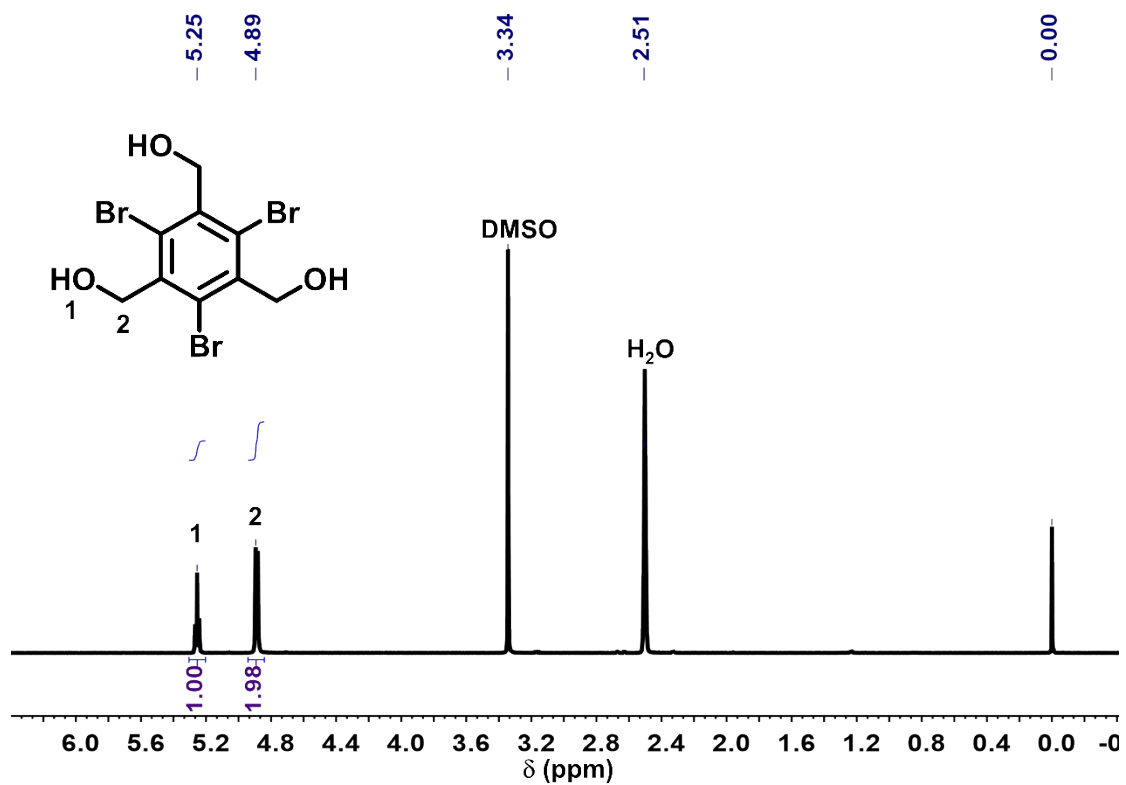


Figure S6. ¹H NMR (400 MHz) spectrum of compound C in DMSO.

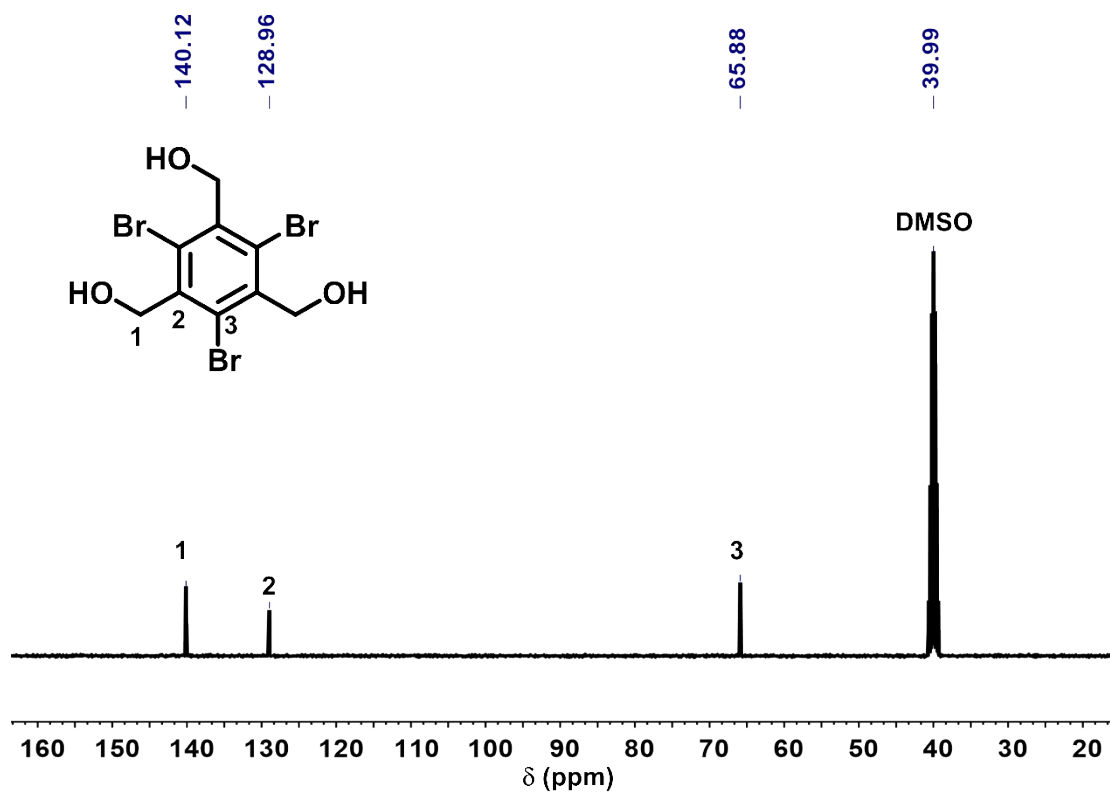


Figure S7. ¹³C NMR (100 MHz) spectrum of compound C in DMSO.

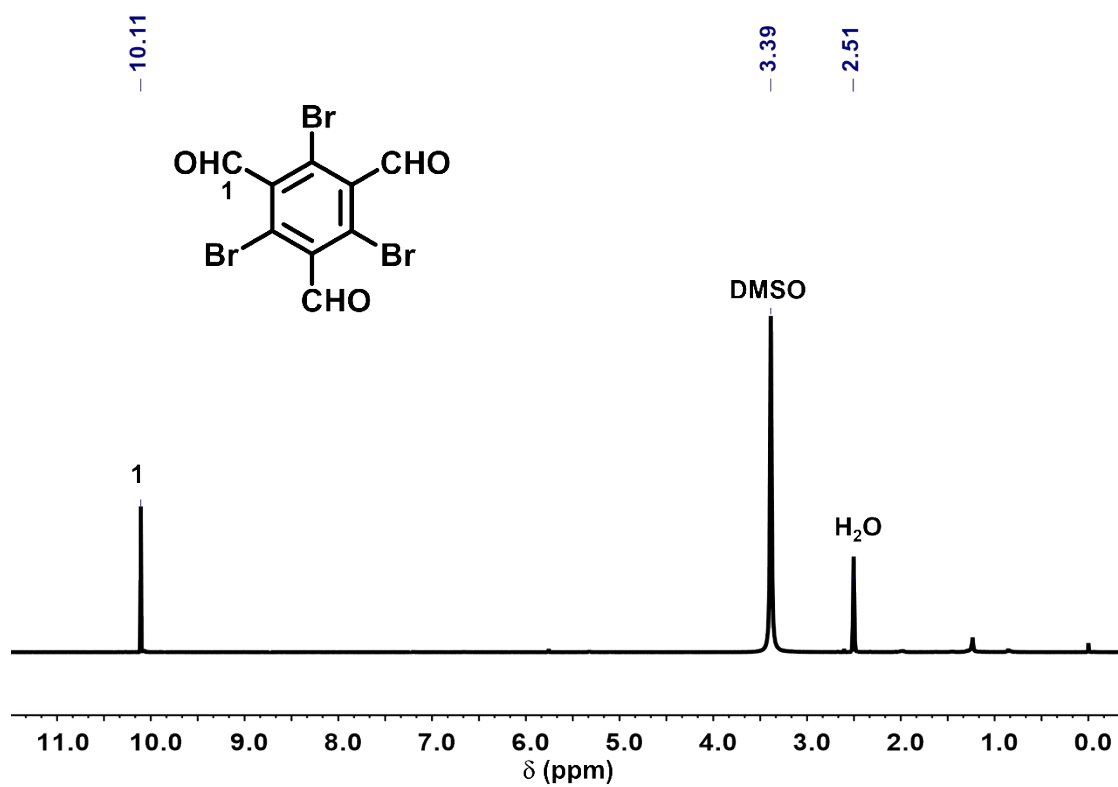


Figure S8. $^1\text{H NMR}$ (400 MHz) spectrum of compound **D** in DMSO.

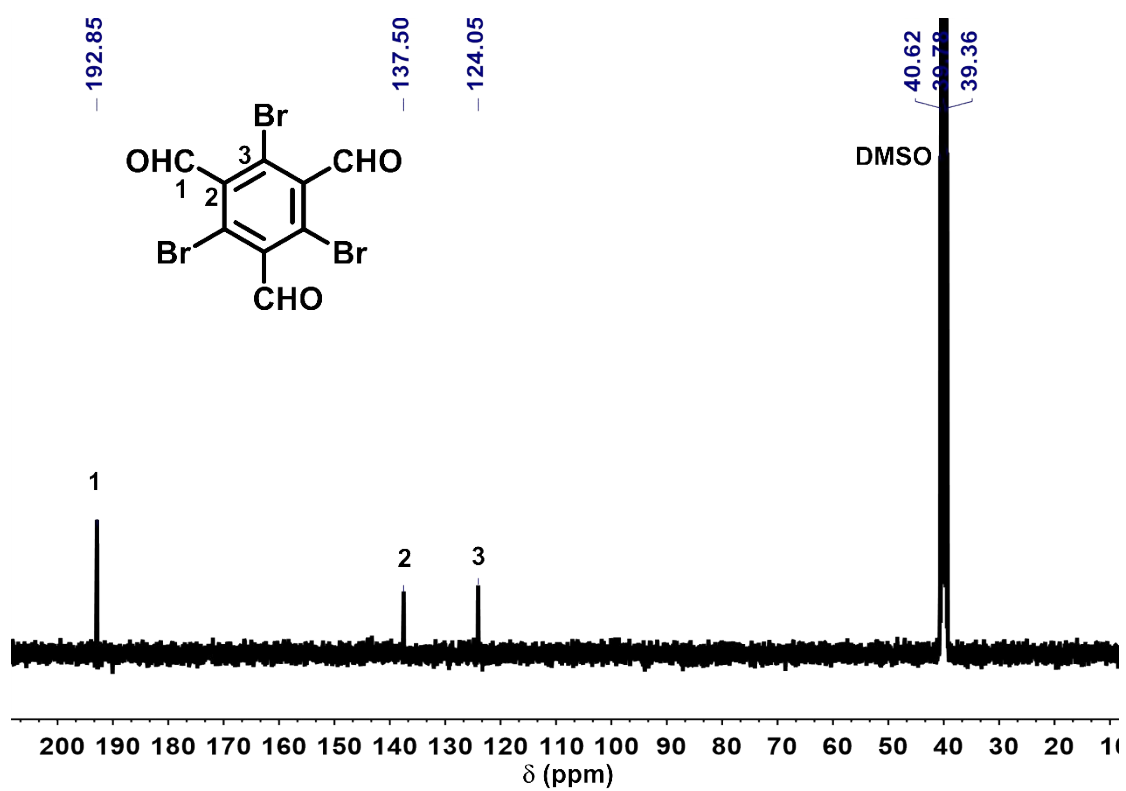


Figure S9. $^{13}\text{C NMR}$ (100 MHz) spectrum of compound **D** in DMSO.

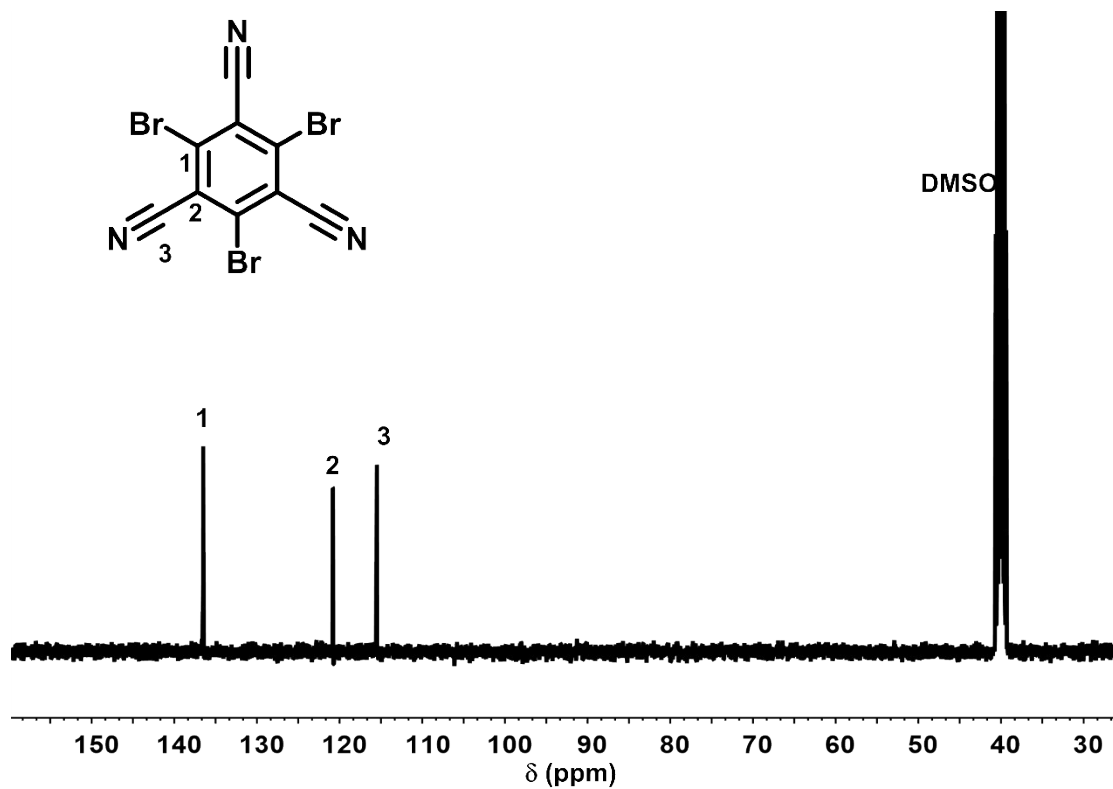


Figure S10. ^{13}C NMR (100 MHz) spectrum of compound F in DMSO.

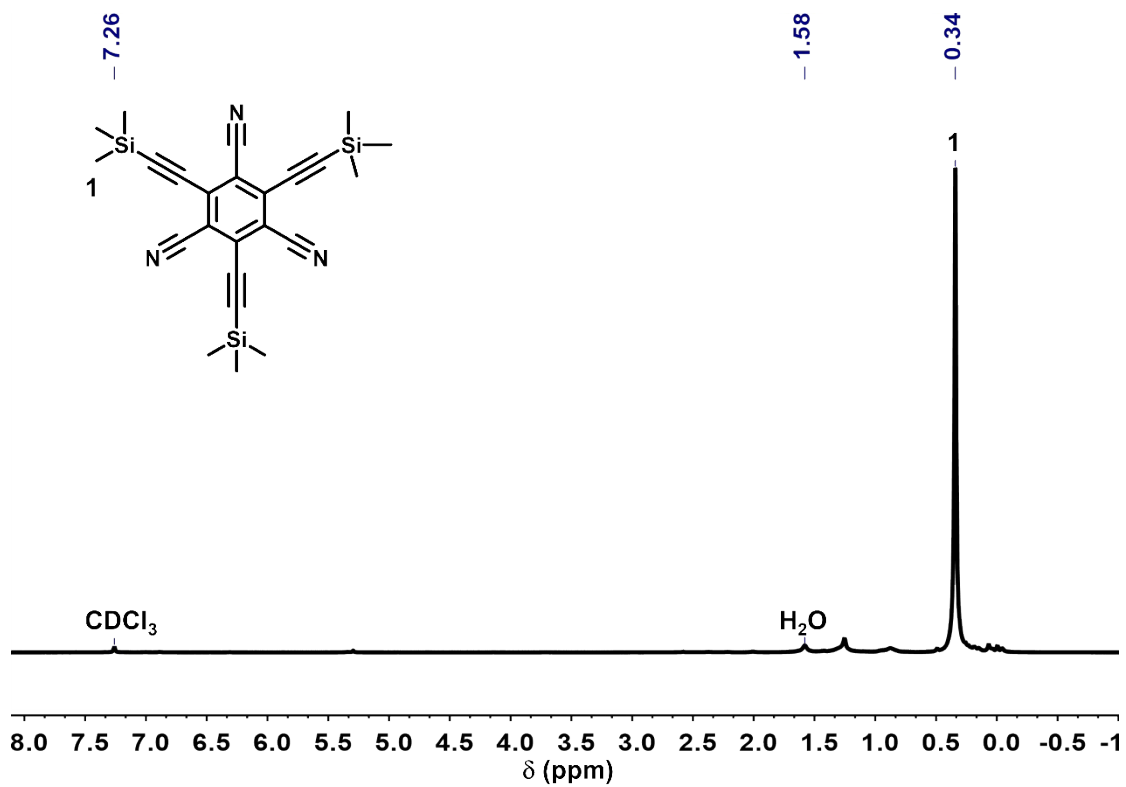


Figure S11. ^1H NMR (400 MHz) spectrum of compound G in CDCl_3 .

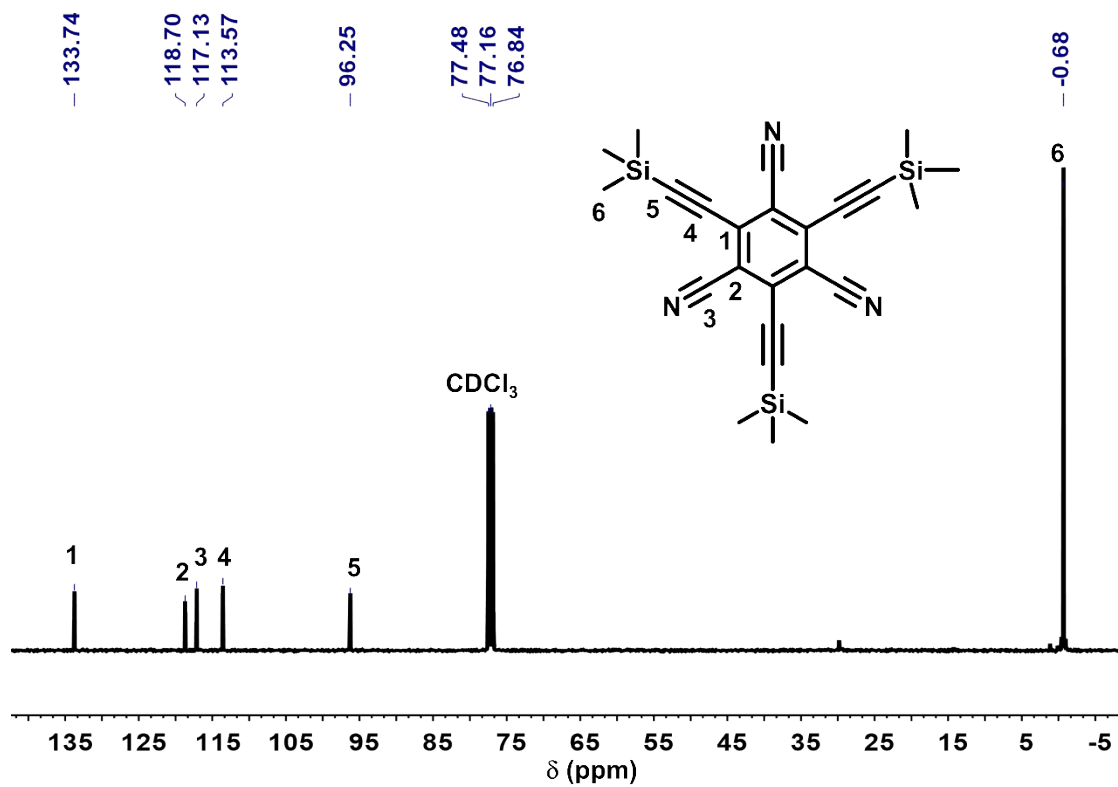


Figure S12. ^{13}C NMR (100 MHz) spectrum of compound **G** in CDCl_3 .

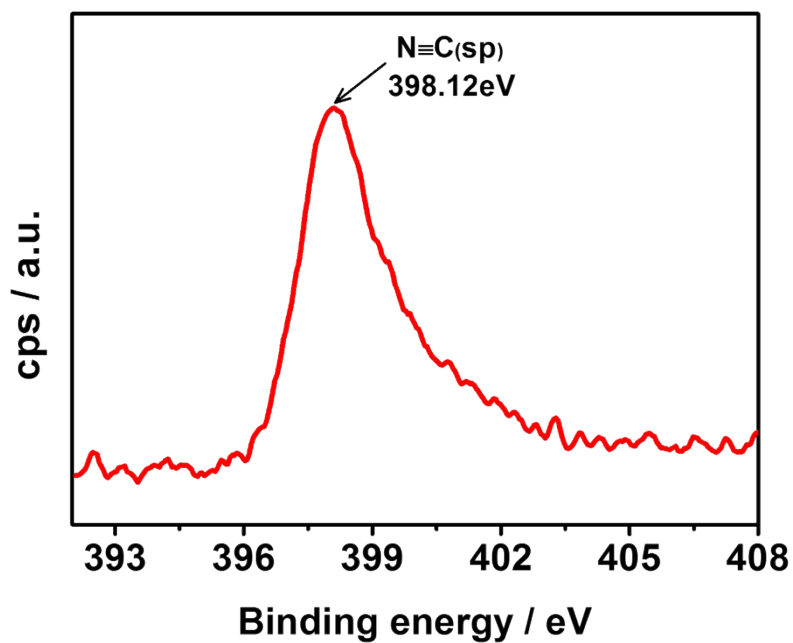


Figure S13. High resolution $\text{N } 1\text{s}$ XPS spectra of CN-GDY on HMDS modified

SiO_2/Si .

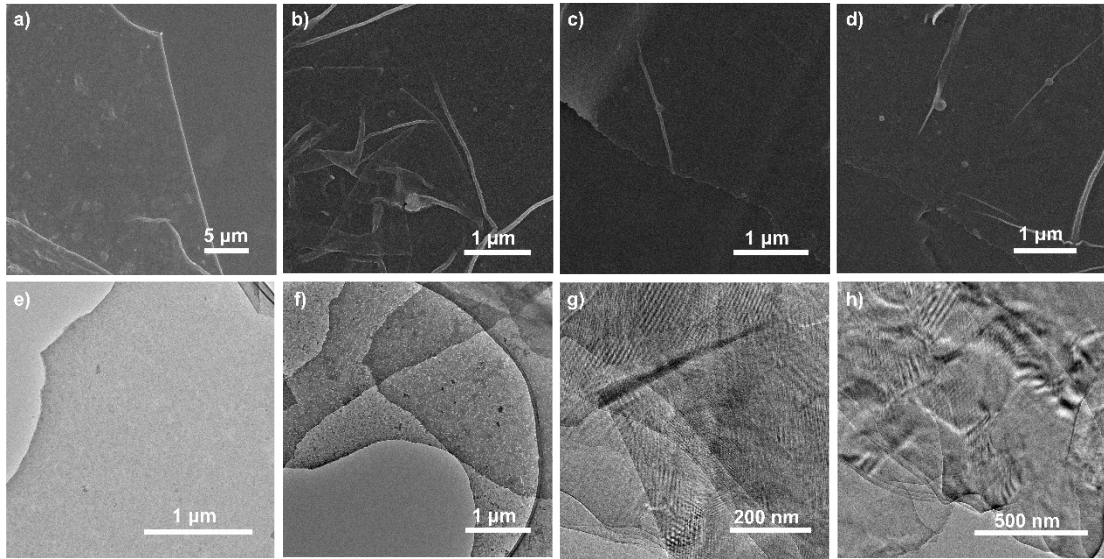


Figure S14. a-d SEM images of CN-GDY; e-h TEM images of CN-GDY.

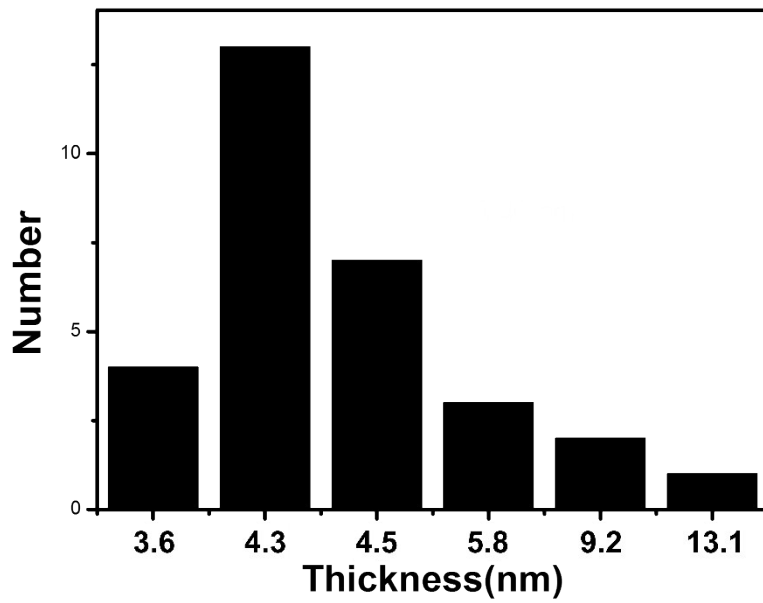


Figure S15. Thickness statistics of 30 flakes of CN-GDY samples.

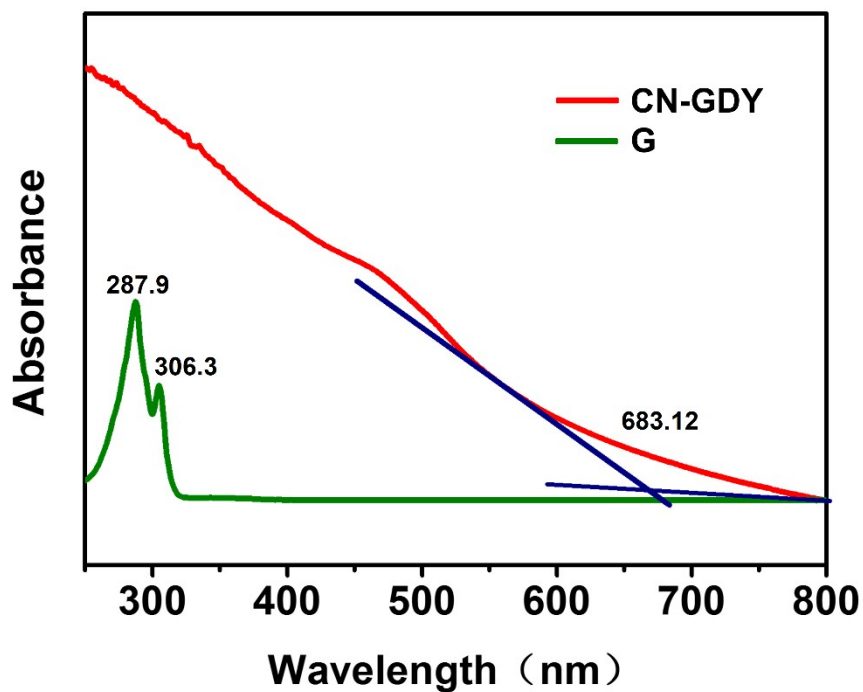


Figure S16. UV-vis spectrum of the compound **G** and **CN-GDY**.

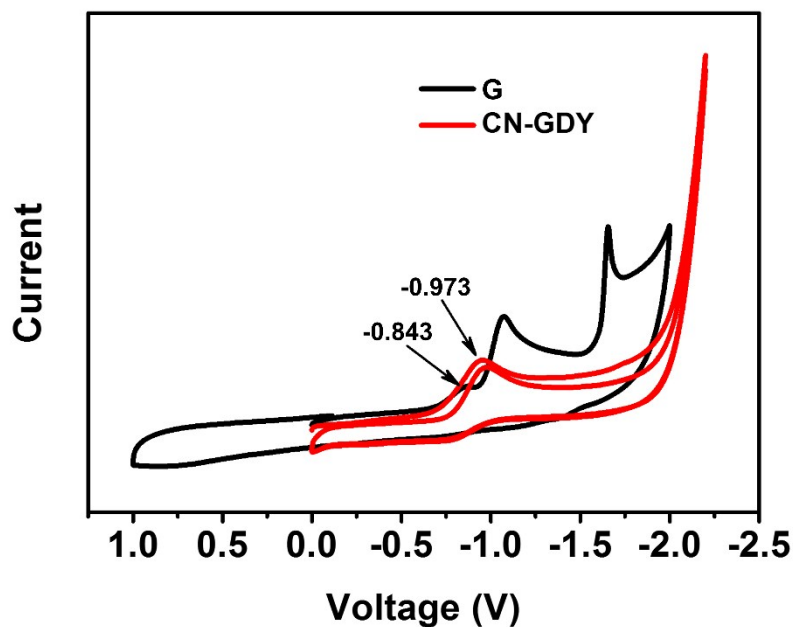


Figure S17. Cyclic voltammograms (CV) of the compound **G** and **CN-GDY** (recorded at a scan rate of 0.1 mV/s 100 mV/s in 0.1 M tetrabutylammoniumhexafluorophosphate (TBAPF₆)/CH₂Cl₂ electrolyte).

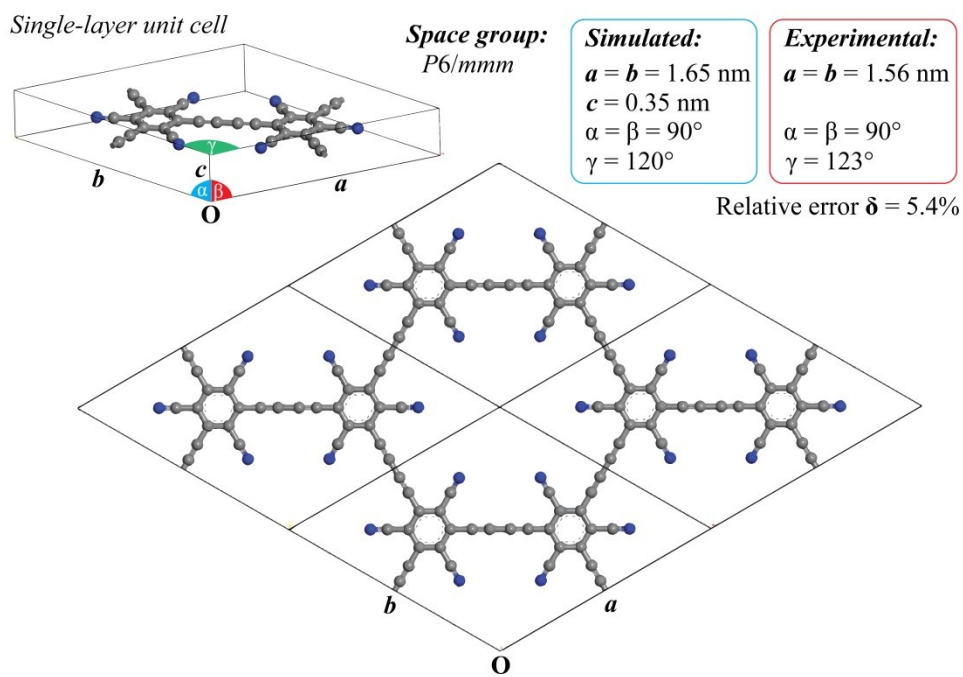


Figure S18. The mono-layer model obtained by the Forcite module in Materials Studio software packages.

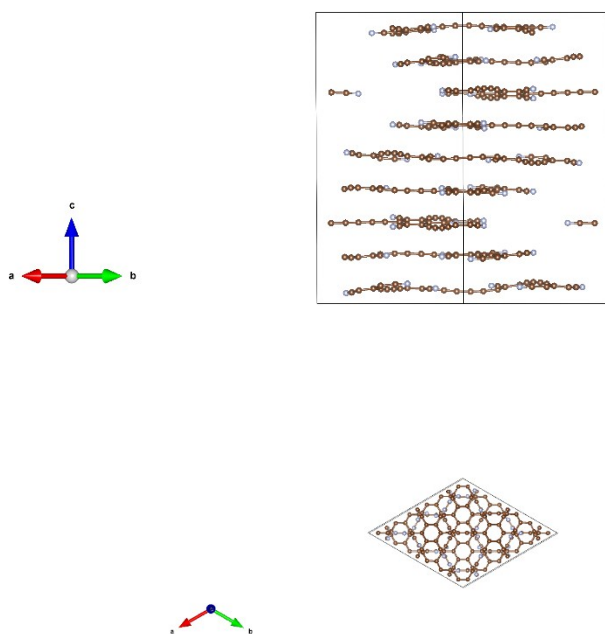


Figure S19. Side and top views of CN-GDY.

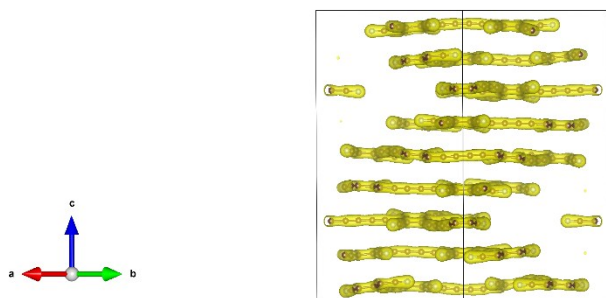


Figure S20. Total charge density distribution with an isovalue of 0.16 electrons/bohr³ for the isosurfaces.

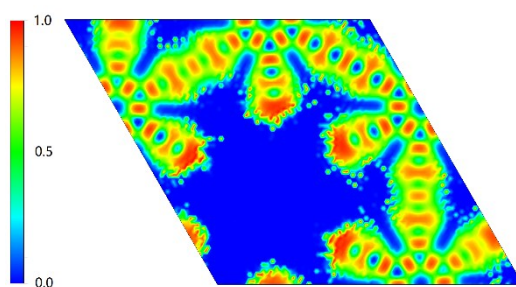
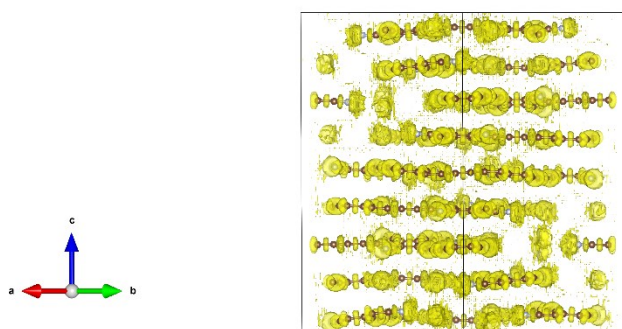


Figure S21. The electron localization function for CN-GDY (001) surface. The values less than 0.5 where one expects the electrons to be delocalized (blue in the figure), and values between 0.5 and 1.0 in regions that can be ascribed to bonding and non-bonding localized electrons.

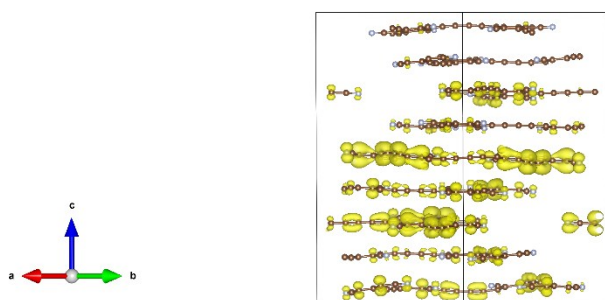


Figure S22. Side views of the partial density for the top of the valence band with an isovalue of 0.0005 electrons/bohr³.

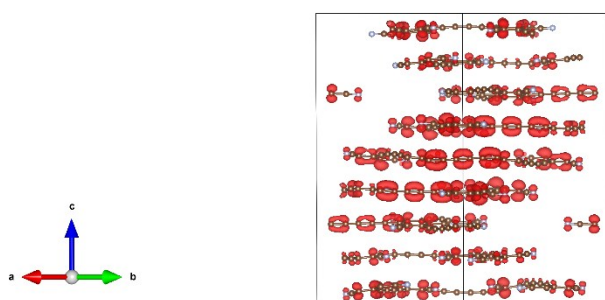


Figure S23. Side views of the partial density for the bottom of the conduction band with an isovalue of 0.0005 electrons/bohr³.

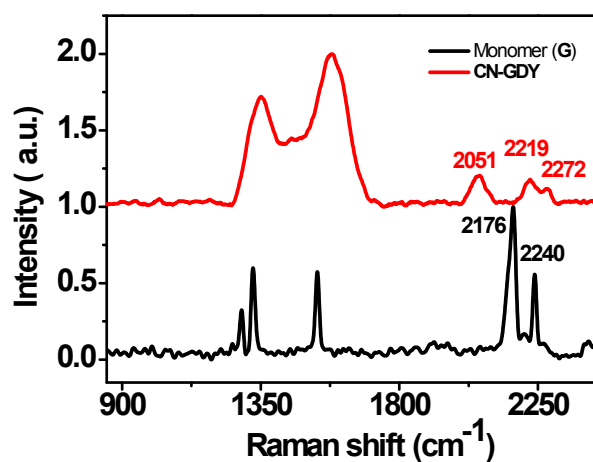


Figure S24. Raman spectras of the compound **G** and **CN-GDY**.